Synthesis of Li_2NH Hollow Nanospheres with Superior Hydrogen Storage Kinetics by Plasma Metal Reaction

Lei Xie,[†] Jie Zheng,[†] Yang Liu,[†] Yan Li,[†] and Xingguo Li*[,†,‡]

Beijing National Laboratory for Molecular Sciences (BNLMS) (The State Key Laboratory of Rare Earth Materials Chemistry and Applications), College of Chemistry and Molecular Engineering, Peking University, Beijing 100871, China, and College of Engineering, Peking University, Beijing 100871, China

Received June 6, 2007. Revised Manuscript Received October 16, 2007

Li_2NH hollow nanospheres were prepared by plasma metal reaction based on the Kirkendall effect. In this synthesis, the bulk lithium was vaporized and reacted with ammonia to obtain the hollow nanostructure directly. The electron microscopy results suggested that more than 90% of the obtained hollow nanospheres were in the range 100–200 nm, and the thickness was about 20 nm. In addition, the BET measurement indicated that the specific surface area of the Li_2NH hollow nanospheres was 79 m^2/g. Because of its short diffusion distance and large specific surface area, the novel structure enhanced the hydrogen storage kinetics of Li_2NH dramatically. It was found that the obtained sample could absorb 6.0 wt % hydrogen in 1 min at 473 K, and the desorption temperature decreased about 115 K compared with the bulk sample. In addition, the effect of novel structure on hydrogen storage kinetics was discussed.

Introduction

Materials with nanoscale hollow structure have attracted considerable attention due to their novel structure and diverse potential applications such as drug delivery,[1] catalysis,[2] plasmon devices,[3] and structural materials.[4] The common method to synthesize hollow materials is using a sacrificed template, such as silica spheres,[5] carbon nanoparticles,[6] and polystyrene beads.[7] These synthetic approaches usually involve a multistep process including fabricating a template, coating with a shell, and removal of the template. Recently, a method to fabricate hollow nanospheres was developed based on the Kirkendall effect associated with different diffusion rates of the atoms moving in and out of the sphere.[8]

The diffusion rate of lithium atom is faster than some elements because of the low melting point and small atom radii of lithium. Therefore, a large quantity of vacancies may be formed during the formation of lithium-based compounds due to the Kirkendall effect. When the particle size of lithium is confined into nanometer scale, the vacancies may assemble quickly and fabricate hollow nanostructure.[8a] At present, lithium imide is receiving increasing attention due to its high hydrogen storage capacity and low operative temperature.[9] However, its poor hydrogen storage kinetics limits its practical use. In order to improve its hydrogen storage properties, much attention has been focused on mechanical ball milling activation,[10] doping with catalyst,[11] or forming new metal–N–H compounds by partial cation substitution.[9b,c] Recent study indicated that both the lithium amide/lithium imide decomposition and hydrogenation processes were dependent on the migration of Li^+ and H^+ ions in the bulk phase and the Li^+ concentration on the surface.[12] Decreasing the diffusion distance to nanometers and increasing the specific surface area are beneficial to improve the hydrogen

* To whom correspondence should be addressed. E-mail: xgl@pku.edu.cn.
† College of Chemistry and Molecular Engineering.
‡ College of Engineering.

(1) (a) Mathiowitz, E.; Jacob, J. S.; Jon, Y. S.; Carino, G. P.; Chickering, D. E.; Chaturvedi, P.; Santos, C. A.; Vijayaraghavan, K.; Montgomery, S.; Bassett, M.; Morrell, C. *Nature (London)* **1997**, *386*, 410–414. (b) Marinakos, S. M.; Novak, J. P.; Brousseau, L. C.; House, A. B.; Edeki, E. M.; Feldhaus, J. C.; Feldheim, D. L. *J. Am. Chem. Soc.* **1999**, *121*, 8518–8522.

(2) (a) Kim, S. W.; Kim, M.; Lee, W. Y.; Hyeon, T. *J. Am. Chem. Soc.* **2002**, *124*, 7642–7643. (b) Dhas, N. A.; Suslick, K. S. *J. Am. Chem. Soc.* **2005**, *127*, 2368–2369. (c) Chen, G.; Xia, D. G.; Nie, Z. R.; Wang, Z. Y.; Wang, L.; Zhang, L.; Zhang, J. J. *Chem. Mater.* **2007**, *19*, 1840–1844.

(3) (a) Sun, Y. G.; Mayers, B.; Xia, Y. N. *Adv. Mater.* **2003**, *15*, 641–646. (b) Lu, X. M.; Tuan, H. Y.; Chen, J. Y.; Li, Z. Y.; Korgel, B. A.; Xia, Y. N. *J. Am. Chem. Soc.* **2007**, *129*, 1733–1742.

(4) (a) Cochran, J. K. *Curr. Opin. Solid. State Mater.* **1998**, *3*, 474–479. (b) Andersen, O.; Waag, U.; Schneider, L.; Stephani, G.; Kieback, B. *Adv. Eng. Mater.* **2000**, *2*, 192–195.

(5) (a) Caruso, F.; Caruso, R. A.; Mohwald, H. *Science* **1998**, *282*, 1111–1114. (b) Caruso, F. *Chem.—Eur. J.* **2000**, *6*, 413–419. (c) Peng, Q.; Dong, Y. J.; Li, Y. D. *Angew. Chem., Int. Ed.* **2003**, *42*, 3027–3030.

(6) (a) Sun, X. M.; Li, Y. D. *Angew. Chem., Int. Ed.* **2004**, *43*, 3827–3831. (b) Li, X. L.; Lou, T. J.; Sun, X. M.; Li, Y. D. *Inorg. Chem.* **2004**, *43*, 5442–5449. (c) Bang, J. H.; Suslick, K. S. *J. Am. Chem. Soc.* **2007**, *129*, 2242.

(7) (a) Zhong, Z. Y.; Yin, Y. D.; Gates, B.; Xia, Y. N. *Adv. Mater.* **2000**, *12*, 206. (b) Caruso, R. A.; Susha, A.; Caruso, F. *Chem. Mater.* **2001**, *13*, 400–409.

(8) (a) Yin, Y. D.; Rioux, R. M.; Erdonmez, C. K.; Hughes, S.; Somorjai, G. A.; Alivisatos, A. P. *Science* **2004**, *304*, 711–714. (b) Gao, J. H.; Liang, G. L.; Zhang, B.; Kuang, Y.; Zhang, X. X.; Xu, B. *J. Am. Chem. Soc.* **2007**, *129*, 1428–1433. (c) Yin, Y. D.; Erdonmez, C. K.; Cabot, A.; Hughes, S.; Alivisatos, A. P. *Adv. Funct. Mater.* **2006**, *16*, 1389–1399.

(9) (a) Chen, P.; Xiong, Z. T.; Luo, J. Z.; Lin, J. Y.; Tan, K. L. *Nature (London)* **2002**, *420*, 302–304. (b) Xiong, Z. T.; Wu, G. T.; Hu, H. J.; Chen, P. *Adv. Mater.* **2004**, *16*, 1522. (c) Leng, H. Y.; Ichikawa, T.; Hino, S.; Hanada, N.; Isobe, S.; Fujii, H. *J. Phys. Chem. B* **2004**, *108*, 8763–8765. (d) Hu, Y. H.; Ruckenstein, E. *J. Phys. Chem. A* **2003**, *107*, 9737–9739. (e) Lu, J.; Fang, Z. Z.; Sohn, H. Y. *J. Phys. Chem. B* **2006**, *110*, 14236–14239.

(10) Markmaitree, T.; Ren, R.; Shaw, L. L. *J. Phys. Chem. B* **2006**, *110*, 20710–20718.

(11) Ichikawa, T.; Isobe, S.; Hanada, N.; Fujii, H. *J. Alloys Compd.* **2004**, *365*, 271–276.

(12) (a) David, W. I. F.; Jones, M. O.; Gregory, D. H.; Jewell, C. M.; Johnson, S. R.; Walton, A.; Edwards, P. P. *J. Am. Chem. Soc.* **2007**, *129*, 1594–1601.

10.1021/cm071517d CCC: $40.75
Published on Web 12/08/2007

storage kinetics. In this paper, we have synthesized Li_2NH in hollow nanosphere structure by plasma metal reaction based on the Kirkendall effect. The novel structure enhances the hydrogen storage kinetics of Li_2NH dramatically.

Experimental Section

A schematic illustration of the experimental equipment for the production of Li_2NH hollow nanospheres is presented in the Supporting Information. It mainly consists of a reaction chamber and a collecting room. In order to transfer samples synthesized in the reaction chamber to the collecting room conveniently, a circulation pump is equipped between them. The collecting room is located in an Ar-filled glovebox. First, about 10 g of bulk lithium (purity >99.9%) was put in the reaction chamber, and then the chamber was evacuated to 0.01 Torr. Second, a mixture of Ar (50%) and NH_3 (50%) at 560 Torr was introduced to the equipment. Finally, the bulk lithium was arc melted with an arc voltage of 25 V and an arc current of 150 A. The flow rate of the circulation gas of Ar and NH_3 for collection of the product was about 100 L/min. The distance between the bulk lithium and electrode was kept at 1 cm, and the system pressure was maintained at 560 Torr. The product was cooled to room temperature after the reaction was stopped. After that, the equipment was evacuated to vacuum and then filled with 760 Torr of Ar for sample collection. The samples before characterization were always handled in a Ar atmosphere in order to minimize their oxidation and hydrolyzation.

The structural analysis of the samples was carried out by X-ray diffraction (XRD) using an automated Rigaku X-ray diffractometer with monochromatic Cu Kα radiation. The size distribution and morphology of the samples were observed by transmission electron microcopy (TEM) using a JEM-200CX operating at 160 kV and scanning electron microscopy (SEM) using a Hitachi S4800 at 10 kV. The BET measurement was operated by absorbing/desorbing nitrogen at 77 K after outgas in vacuum at 453 K for 1 h on a COULTER SA 3100. The Fourier transform infrared spectroscopy (FTIR) measurements were performed by SHIMADZU FTIR-8400. The X-ray photoelectron spectroscopy (XPS) measurements were taken on an AXIS-Ultra instrument from Kratos Analytical using monochromatic Al Kα radiation (225 W, 15 mA, 15 kV) and low-energy electron flooding for charge compensation. To compensate for surface charges effects, binding energies were calibrated using C 1s hydrocarbon peak at 284.80 eV. The data were converted into VAMAS file format and imported into CasaXPS software package for manipulation and curve fitting.

The differential scanning calorimetry (DSC) was performed on a Netzsch DSC 204 HP calorimeter at a heating rate of 10 K/min. The absorption measurement was operated under 35 bar of H_2 directly. The desorption was measured under 1 bar of Ar after the samples were heated at 573 K under 35 bar of H_2 for 1 h and then cooled to room temperature. In both cases, the gas flow rate was about 50 mL/min.

Isotherm measurements were conducted to obtain PCT curves and hydrogen sorption kinetics curves at different temperatures. During the sorption kinetics measurements, the hydrogen pressure is about 35 bar. The sample mass for each hydrogen absorption measurement was about 0.1 g. All the equipments must be vacuumed before introducing hydrogen in each measurement. In addition, hydrogen detection apparatus should be fixed along the measurement equipment.

Results and Discussion

The size distribution and morphology of the samples were investigated by electron microscopy. Figure 1a,b shows that the product is in hollow nanostructure, and the diameters range from 100 to 400 nm with more than 90% in the range

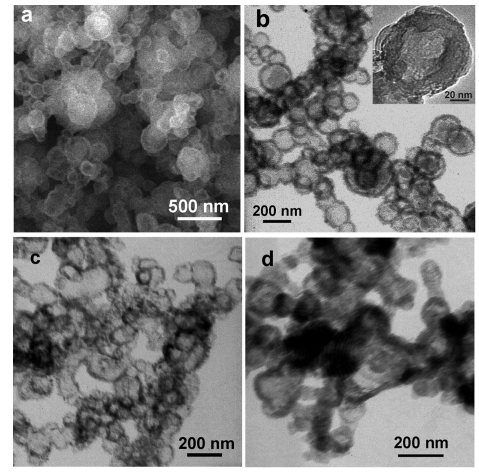

Figure 1. (a) SEM image, (b) TEM image (inset: magnified TEM image) of the as-prepared Li_2NH hollow nanospheres, (c) TEM image of the Li_2NH hollow nanospheres annealing at 573 K under vacuum for 1 h, and (d) TEM image of the Li_2NH hollow nanospheres after hydrogenated at 573 K under 35 bar of hydrogen for 1 h.

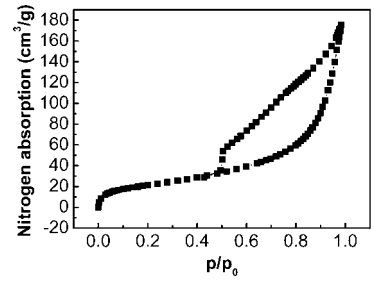

Figure 2. BET pattern of Li_2NH hollow nanospheres.

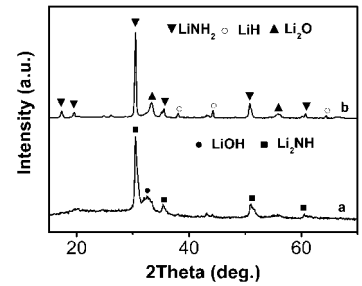

Figure 3. XRD patterns of (a) Li_2NH hollow nanospheres and (b) Li_2NH hollow nanospheres after hydrogenated at 573 K under 35 bar of hydrogen for 1 h.

100–200 nm. The inset of the Figure 1b shows a magnified image of a typical hollow nanosphere about 120 nm. The shell thickness is about 20 nm. It is interesting that the nanometer hollow structure can survive on an annealing temperature as high as 573 K, as indicated in Figure 1c. Figure 1d shows that even after being hydrogenated at 573 K under 35 bar of hydrogen for 1 h, the hollow structure is maintained, except that the interfaces of the hollow nanospheres become a little ambiguous. The BET measurement shown in Figure 2 indicates that the specific surface area of the Li_2NH hollow nanospheres is 79.4 m^2/g.

The XRD pattern shown in Figure 3a indicates that the as-prepared sample mainly comprises of Li_2NH (JCPDS 75-0050) and a small amount of LiOH. The reaction path can be expressed as eq 1. Determined by the Scherrer equation, the crystallite sizes of Li_2NH hollow nanospheres is about

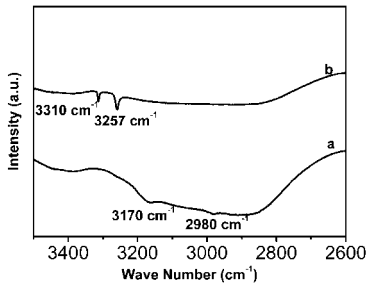

Figure 4. FTIR spectra results of (a) Li_2NH hollow nanospheres and (b) Li_2NH hollow nanospheres after hydrogenated at 573 K under 35 bar of hydrogen for 1 h.

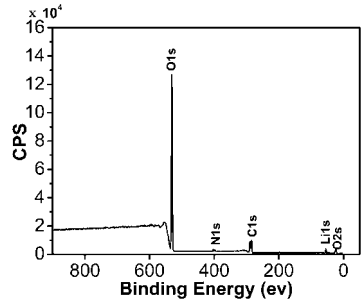

Figure 5. XPS results of the Li_2NH hollow nanospheres.

Scheme 1. Formation Mechanism of the Li_2NH Hollow Nanospheres

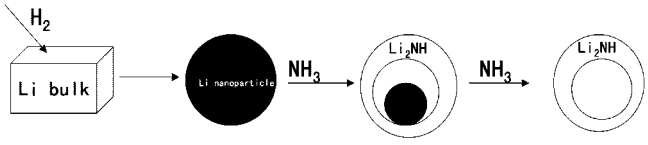

15 nm. This result indicates that small nanocrystals are assembled together in the shell of the hollow nanospheres. Figure 3b shows that, after the Li_2NH hollow nanospheres hydrogenated at 573 K under 35 bar of hydrogen for 1 h, the main phase changes to $LiNH_2$ (JCPDS 75-0049) and LiH (JCPDS 78-0039), which accords to eq 2.

$$2Li + NH_3 \rightarrow Li_2NH + H_2 \quad (1)$$

$$Li_2NH + H_2 \rightarrow LiNH_2 + LiH \quad (2)$$

The FTIR spectra measurements of the obtained samples are performed, as shown in Figure 4. The peak around 3170 cm^{-1} corresponds to N–H stretches of Li_2NH, and the broad peak around 2980 cm^{-1} corresponds to O–H stretches. After hydrogenation, the peak corresponding to O–H stretches disappears, and two new peaks around 3257 and 3310 cm^{-1} which correspond to N–H stretches of $LiNH_2$ are formed. These results are consistent with the XRD results.

The XPS results shown in Figure 5 indicate that there are Li, O, and N elements on the surface. According to the peak areas of elemental lines after background subtraction and sensitivity factors consideration, the weight percentages of the Li, O, and N element is 33.13%, 46.12%, and 3.1%, respectively. Combined with the XRD results, it can be concluded that the surface of the nanoparticles is mainly composed of LiOH. Because the total quantity of LiOH is small in the product, the hydroxide phase mainly distributes on the surface. The formation of LiOH is mainly due to contamination of the sample with trace of water during the measurements.

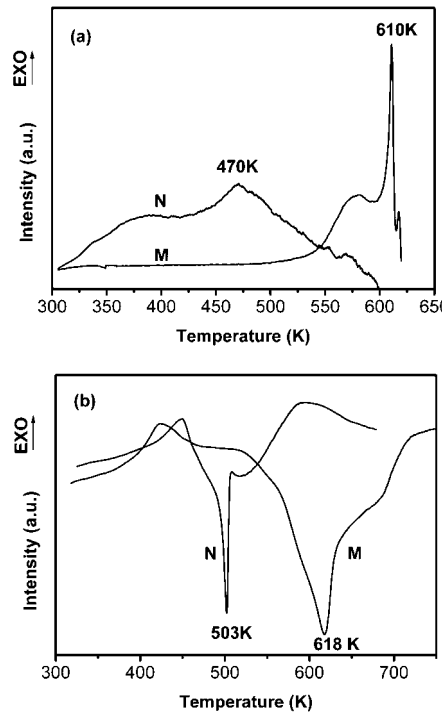

Figure 6. (a) DSC curves of hydrogenation at a heating rate of 10 K/min under 35 bar of H_2 and (b) DSC curves of desorption at a heating rate of 10 K/min under flowing Ar after hydrogenated under 35 bar of H_2 at 573 K for 1 h. N = Li_2NH hollow nanospheres, and M = Li_2NH micrometer particles.

For comparison, if there is no NH_3 in the chamber, the bulk lithium is vaporized so slowly that almost no product can be formed. However, if the NH_3 is changed to H_2, the bulk lithium can be vaporized. The improved evaporation rate may be ascribed to the effect of H_2.[13] (In the NH_3 atmosphere, a little amount of H_2 is formed during the arc discharge process.) Determined from the results, the formation mechanism of Li_2NH hollow nanospheres might be expressed as Scheme 1. After the lithium vapor is formed, it condenses into nanoscale liquid droplets near the arc region. As the temperature cools, the formed lithium droplets react with NH_3 quickly to form the products. Lithium atoms move faster during such reaction, which induces a large number of vacancies in the phase. In addition, because the lithium liquid droplets are confined into nanoscale core, the net rate of vacancies increases markedly and the supersaturated vacancies are coalesced into a single void.

The hydrogen storage properties of the Li_2NH hollow nanospheres are investigated. In addition, Li_2NH micrometer particles prepared by heating commercial $LiNH_2$ powder in vacuum at 623 K for 10 h were included as a reference sample. Figure 6a suggests that the Li_2NH micrometer particles start to absorb hydrogen at 550 K, and the peak temperature is about 610 K. However, the Li_2NH hollow nanospheres start to absorb hydrogen at room temperature,

(13) (a) Ohno, S. *Koon Gakkaishi* **1993**, *19*, 105–111. (b) Okuyama, H.; Ohno, S.; Homma, K.; Ozawa, M.; Uda, M. *Koon Gakkaishi* **1989**, *15*, 143–150.

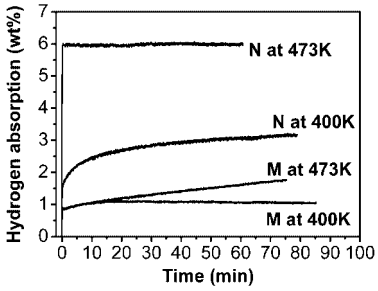

Figure 7. Hydrogenation absorption curves of the obtained samples at different temperature under an initial hydrogen pressure about 35 bar of H_2 of (N) Li_2NH hollow nanospheres and (M) Li_2NH micrometer particles.

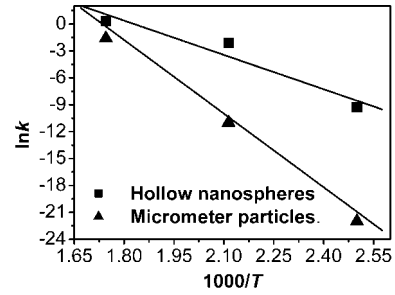

Figure 8. Plot of ln k vs $1000/T$ of the Li_2NH hollow nanospheres and Li_2NH micrometer particles.

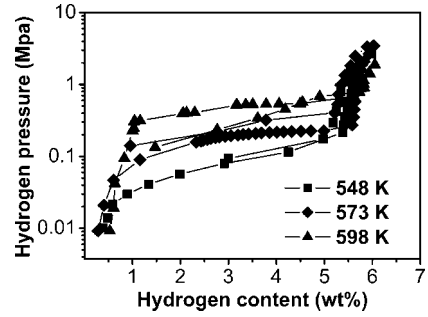

Figure 9. PCT curves of the Li_2NH hollow nanospheres at different temperatures.

and the peak temperature is about 470 K. In addition, the hydrogen desorption temperature of Li_2NH reduces dramatically. From Figure 6b it can be seen that the onset and peak of temperature of the hydrogenated Li_2NH micrometer particles are 571 and 618 K, respectively, while of the hydrogenated Li_2NH hollow nanospheres are 452 and 503 K. The obtained results suggest that the novel structure of hollow nanospheres decreases the operative temperatures significantly compared to the micrometer sample. Some former researches have suggested that the initial absorption temperature was 500 K and the initial desorption temperature was 550 K in an argon atmosphere upon heating.[9a,14] Furthermore, the peak temperature of desorption decreased to 510 K only after it doped with $TiCl_3$ by the milling method.[11]

Not only do the operating temperatures decrease obviously, but also the absorption rate increases dramatically. As shown in Figure 7, the Li_2NH micrometer particles absorb only 1.6 wt % hydrogen in 1 h at 473 K. However, the hollow nanospheres sample can absorb 6.0 wt % in 1 min at the same temperature. Even at 400 K the hollow nanospheres can absorb 3.0 wt % hydrogen in 1 h while the micrometer particles can absorb only 1 wt % hydrogen in the same time. In addition, the activation energy of absorption is estimated by combined the Johnson–Mehl–Avrami equation with the Arrhenius equation after fitting the experimental data, in which the absorption data at 573 K are added. The rate constant k is determined by eq 3,

$$\log[-\ln(1-f)] = \eta \log k + \eta \log t \qquad (3)$$

where f is the growing phase fraction, t is absorption time, and η is the reaction order. A plot of $\log[-\ln(1-f)]$ vs $\log t$ yields η and $\eta \log k$ when $t = 1$. Then the temperature dependence of k can be correlated by the Arrhenius equation $k = A \exp(-E_a/RT)$, where A is a temperature-independent coefficient, E_a is the activation energy, R is the gas constant, and T is the absolute temperature. The plot of ln k vs $1000/T$ is shown in Figure 8. From the obtained results, the activation energy of absorption of the Li_2NH micrometer particles and hollow nanospheres is 225 and 106 kJ/mol, respectively. As the ball milled sample with $TiCl_3$, the activation energy is about 110 kJ/mol.[11]

It is generally considered that physical and chemical properties can be developed obviously when downsizing materials into nanoscale range. The dramatically enhanced hydrogen storage kinetics can be attributed to larger specific surface area and shorter diffusion distance of the nanometer hollow structure. In the hydrogenation process, absorption kinetics is dominated by Li^+ concentration on the surface and migration of H^+ in the bulk phase.[12] As the hollow nanospheres structure formed, the proportion of the total number of Li^+ on the surface increases, which makes Li_2NH able to absorb H_2 more actively. After hydrogen molecules reacting with Li^+ cations, LiH and protonic hydrogen are formed. Then the protonic hydrogen migrates to the bulk phase to complete the hydrogenation.[12] The hollow nanostructure decreases the diffusion distance considerably because that the shell thickness is only about 20 nm. Therefore, the novel structure enhances the absorption kinetics significantly due to two factors. In the dehydrogenation process, desorption kinetics depends on migration of Li^+ ions and interaction of LiH and $LiNH_2$ phases.[9b,12] From the above results we know that the formed LiH and $LiNH_2$ phases maintain in the nanometer hollow structure. Besides that the nanometer hollow structure facilitates the migration of Li^+ ions, the nanoscale distance between $LiNH_2$ and LiH domains promotes the desorption reaction. Therefore, the desorption temperature of the hollow nanostructure decreases dramatically compared to the micrometer sample.

Furthermore, PCT curves of the Li_2NH hollow nanospheres at different temperatures were measured, as shown in Figure 9. The plateau pressure is 0.38, 0.22, and 0.11 MPa at 598, 573, and 548 K, respectively. Calculated from the slope of the Van't Hoff equation, the desorption enthalpy of the hydrogenated hollow nanospheres is about 67.9 kJ/mol, which is close to the former results.[9a]

(14) Nakamori, Y.; Orimo, S. *Mater. Sci. Eng., B* **2004**, *108*, 48–50.

Conclusions

In conclusion, a novel and facile method for preparing Li_2NH hollow nanospheres based on the Kirkendall effect was developed. The special nanostructure shows significantly improved hydrogen storage kinetics compared to that of the Li_2NH micrometer particles. The absorption temperature decreases markedly, and absorption rate enhances dramatically because of the larger specific surface area and nanometer diffusion distance in the special hollow nanosphere structure. Meanwhile, the desorption temperature decreases dramatically due to the hydrogenated product $LiNH_2$ and LiH maintaining the hollow nanosphere structure, in which the two phases are limited in the nanometer range. The obtained results suggest that the nanoscale hollow structure improves the hydrogen storage kinetics of lithium imide significantly, which opens up the possibilities that novel structures in nanometers facilitate the kinetics of other hydrogen storage materials. Furthermore, this synthetic method would be extended to preparation of other inorganic compounds with hollow nanospheres structure and can be scale up for industrial need.

Acknowledgment. This work was supported by the National Natural Science Foundation of China (Nos. 20221101, 10335040, and 20671004) and MOST of China (No. 2006AA05Z130).

Supporting Information Available: Schematic illustration of the experimental equipment. This material is available free of charge via the Internet at http://pubs.acs.org.

CM071517D